Incommensurate Magnetic Fluctuations in $La_{2-x}Sr_xCuO_4$

S-W. Cheong,[1] G. Aeppli,[1] T. E. Mason,[1,2] H. Mook,[3] S. M. Hayden,[4] P. C. Canfield,[5] Z. Fisk,[5] K. N. Clausen,[2] and J. L. Martinez[6]

[1]*AT&T Bell Laboratories, Murray Hill, New Jersey 07974*
[2]*Risø National Laboratory, Roskilde DK-4000, Denmark*
[3]*Oak Ridge National Laboratory, Oak Ridge, Tennessee 37831*
[4]*H. H. Wills Physics Laboratory, University of Bristol, Bristol B58 ITL, United Kingdom*
[5]*Los Alamos National Laboratory, Los Alamos, New Mexico 87545*
[6]*Institut-Laue-Langevin, B.P. 156X, Grenoble 38042, France*

(Received 21 May 1991)

We use inelastic neutron scattering to establish the modulation vectors δ and correlation lengths for the incommensurate magnetic fluctuations in metallic samples of $La_{2-x}Sr_xCuO_4$ with $x=0.075$ and 0.14. In notation appropriate for a square lattice where the magnetic instability in the undoped case occurs at (π,π), the vectors δ are along $(\pi,0)$ and $(0,\pi)$. The correlation length ξ is larger than the distance between carriers, is weakly dependent on x, and changes significantly between 12 and 100 K for both compositions.

PACS numbers: 75.50.Ee, 74.70.Hk, 74.70.Jm, 75.40.Cx

In spite of considerable effort, the nature of the magnetic correlations in the metallic cuprates remains unclear. Theoretical work [1-3] suggests that for small carrier concentrations, there should be antiferromagnetic correlations with a period incommensurate with that of the lattice. Neutron-scattering experiments on $YBa_2Cu_3O_{6+\delta}$ [4] and $La_{2-x}(Ba,Sr)_xCuO_4$ [5,6] show that for small doping, the antiferromagnetic long-range order is replaced by commensurate fluctuations with a correlation length of order of the interimpurity spacing. At higher doping levels, incommensurate fluctuations have been reported [6] for $La_{2-x}Sr_xCuO_4$ but not for $YBa_2Cu_3O_{6+\delta}$. However, because of experimental limitations, the incommensurate wave vector δ and antiferromagnetic correlation length ξ have remained undetermined. To establish δ and ξ, we have used neutron scattering to measure the magnetic response function $\chi''(\mathbf{Q},\omega)$ as a function of both basal-plane components of the momentum transfer $\mathbf{Q}$ for two metallic samples of $La_{2-x}Sr_xCuO_4$. The present paper describes the results, the most notable being that δ is parallel to $(\pi,0)$ and $(0,\pi)$ [in the notation where (π,π) characterizes the order in a square-lattice antiferromagnet] and that ξ is relatively long and weakly dependent on x.

The crystal samples were grown using the CuO flux method ($x=0.075$) and the traveling-solvent floating-zone technique ($x=0.14$). We deduced the alloy compositions from comparison of structural parameters (c/a ratios) established by neutron diffraction on the samples used in our magnetic scattering experiments to those of earlier ceramic samples of known composition [7]. The Sr concentrations so obtained are identical to those estimated from comparing the tetragonal-orthorhombic transition temperatures of the crystals and sintered powders [7].

Samples grown in the manner of our $x=0.075$ crystals have been extensively characterized and shown to exhibit reproducible bulk properties [8]. For $150 \lesssim T \lesssim 300$ K, the basal-plane resistivity $\rho \cong AT$ with $A=2.7\ \mu\Omega$ cm/K, while for $30 \lesssim T \lesssim 100$ K, $\rho \cong \rho_0[1+(T/T_0)^2]$, where $\rho_0=250\ \mu\Omega$ cm and $T_0=175$ K. Magnetic susceptibility measurements suggest that the sample is not a bulk superconductor.

The rarity of large single crystals of $La_{1.86}Sr_{0.14}CuO_4$ precluded cutting smaller specimens from our sample for characterizations as extensive as those for our $x=0.075$ sample. Nevertheless, dc magnetic susceptibility data [9] for the entire sample used in our neutron-scattering experiment indicate a single sharp onset of superconductivity at $T_c=33$ K. Above T_c, an increasing (with T) contribution similar to that for superconducting ceramics [7] with $x \cong 0.15$ dominates the susceptibility. In addition, there is a small Curie term, with an amplitude corresponding to a population of impurity spins with $S=\frac{1}{2}$ and $g=2$ of 8×10^{-3} per formula unit, and an even smaller contribution from a ferromagnetic contaminant, with an ordered moment below $10^{-5}\mu_B$/Cu.

We performed neutron-scattering measurements at the Risø DR-3 and Institut Laue-Langevin (ILL) reactors, using the TAS6 (Risø), IN14 (ILL), and IN12 (ILL) cold-source instruments in double- and triple-axis modes. The experiments are inelastic, meaning that only magnetic fluctuations, and not frozen spin correlations, associated with ordered magnets and spin glasses, are measured. We collected most of our data for 12 K, which is well above the magnetic freezing temperatures reported for $La_{2-x}(Sr,Ba)_xCuO_4$ with $x \geq 0.05$ [5,10]. Thus, our measurements at $T=12$ characterize states without static magnetic order.

Figure 1 shows reciprocal space for a two-dimensional square lattice. Open circles indicate the reciprocal-lattice points, with coordinates $(n2\pi,m2\pi)$. The circled cross represents the additional reciprocal-lattice point (π,π) which appears when antiferromagnetic order doubles the unit cell along the (1,1) direction in real space, as is the case for the CuO_2 planes in La_2CuO_4 [11]. Because our goal is to establish the nature of the short-range magnetic order in $La_{2-x}Sr_xCuO_4$, we concentrate on constant-

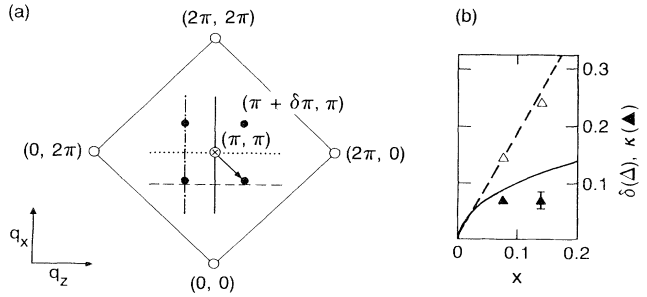

FIG. 1. (a) Reciprocal space for CuO_2 planes. Open circles represent reciprocal-lattice points for the underlying square lattice, the open circle with cross denotes the additional point (π,π) which appears when antiferromagnetic order doubles the unit cell along (1,1) in real space, and solid circles denote the location of peaks in the magnetic response function for metallic $La_{2-x}Sr_xCuO_4$. Solid, dashed, dotted, and dash-dotted lines correspond to different constant-$\hbar\omega$ scans in neutron-scattering experiments. Previous experiments were confined to the solid line, along (π,π). The arrow is the incommensurate vector $\boldsymbol{\delta}=\delta(0,\bar{\pi})$. (b) The dependence of the incommensurability δ and inverse correlation length κ on x, both in notation where $(\pi,0)$ corresponds to unity. Values for $x=0.075$ are obtained from the weighted (by the squared inverse errors) averages of all $T\leq 12$ K data (with $0.65\leq\hbar\omega\leq 5$ meV) described in text. Dashed line represents $\delta=2x$. Solid line represents $\sqrt{x}/\pi$, the mean inverse spacing between carriers (ideally) donated by the Sr atoms to the CuO_2 planes.

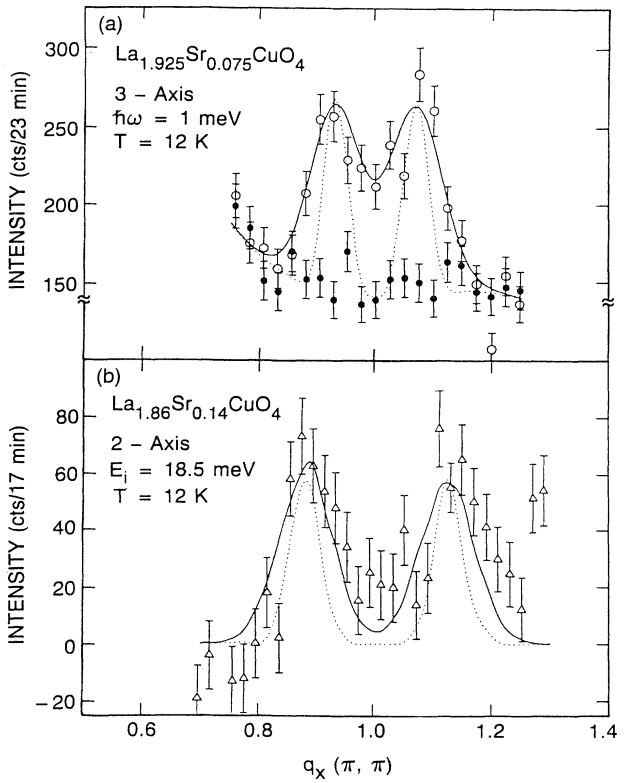

FIG. 2. Scans as a function of q_x where the other basal-plane coordinate $q_z=0.075$ [frame (a)] and $q_z\approx 0.14$ [frame (b)]. Data in frame (a) are for an $x=0.075$ sample and were collected in triple-axis mode with $\hbar\omega$ fixed at 1 meV, $E_f=8.09$ meV, and collimations 133'-50'-110'-150', where the listing proceeds from reactor to detector. Open and solid circles represent uncorrected signal and backgrounds, respectively. Frame (b) shows background-corrected data for $x=0.14$ taken in double-axis mode with $E_i=18.5$ meV and collimations 30'-56'-52'. Solid lines in both (a) and (b) are best fits to data of the function described in text; the dashed line represents instrumental response to δ-function peaks located at $(\pi,\pi)\pm\delta(0,\pi)$ and $\pm\delta(\pi,0)$.

energy-transfer ($\hbar\omega$) surveys of reciprocal space near (π,π). Most of the data were collected for $\hbar\omega=1$ meV$\equiv 0.25\times 10^{12}$ Hz$\equiv 11.6$ K$\ll J$, where $J=0.13$ eV is the exchange constant for La_2CuO_4 [12]. Individual scans through reciprocal space generally follow trajectories similar to those indicated by the dash-dotted, solid, dashed, and dotted lines near (π,π) in Fig. 1. All previous neutron-scattering experiments [6] on $La_{2-x}SrCuO_4$ for $x\neq 0$ have been confined to the solid line, along (π,π). Figure 2(a) shows a typical scan (open circles) of the dash-dotted type, where the momentum transfer q_x along (π,π) is varied with the momentum transfer q_z along $(\pi,\bar{\pi})$ held fixed at 0.075. The solid circles represent the background, determined in an analogous scan with $q_z\cong 0.3$. The data clearly show two peaks at $q_x\cong 0.93$ and 1.07, separated by a minimum at $q_x=1.0$. Thus, the observed incommensurability along (π,π) is comparable to the (fixed) offset q_z along $(\pi,\bar{\pi})$, which suggests that the incommensurate wave vector $\boldsymbol{\delta}$ has a substantial component parallel to $(\pi,\bar{\pi})$. That this is indeed the case is more apparent from Fig. 3, which is a contour plot of the background-corrected data collected on a two-dimensional grid in reciprocal space, labeled by the basal-plane coordinates q_x and q_z. The important features of the data are (i) the overall square symmetry of the scattering with the sides of the square parallel to (π,π) and $(\pi,\bar{\pi})$, and (ii) the accumulation of intensity near the corners of the square. The data also have two more puzzling features, namely, the high intensity at $q_x=1$, $q_z\cong 0.1$, and the slight asymmetry of the pattern around the $q_z=0$ axis. The former is due to a spurious process which disappears on changing the spectrometer configuration (see below), while the latter is due to the instrumental resolution. A theoretical cross section which gives a good description of the data is the sum of four resolution-corrected Gaussians centered at the corners of the square. The corners are displaced by the vectors $\pm\delta(0,\pi)$ and $\pm\delta(\pi,0)$ from (π,π). The best fit to the data is obtained for a wave number $\delta=0.14\pm 0.02$ and an antiferromagnetic correlation length $\xi=2(\text{FWHM})^{-1}=18\pm 1$ Å$=(4.7\pm 0.3)a_0$, where $a_0=3.8$ Å is the nearest-neighbor Cu-Cu separation. Figure 3, right panel, shows the corresponding calculated cross section.

To determine whether $S(Q,\omega)$ depends significantly on $\hbar\omega$, we have accumulated data on a somewhat coarser

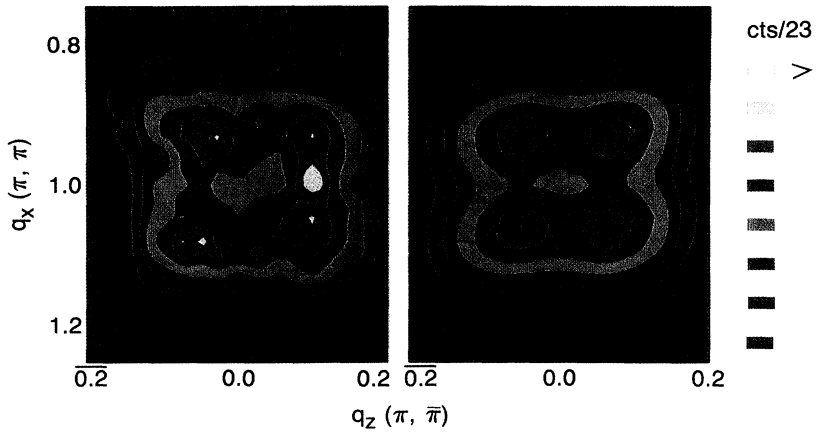

FIG. 3. Contour plots of background-corrected scattering (left) collected at fixed $\hbar\omega = 1$ meV for $x = 0.075$ with spectrometer configuration specified in the caption of Fig. 2(a), and the resolution-corrected theoretical cross section (right) which best describes the data.

grid for $\hbar\omega = 5$ meV. The four-Gaussian form which describes the $\hbar\omega = 1$ meV data also gives a good account of the $\hbar\omega = 5$ meV results. In particular, the fitted values of δ and ξ are indistinguishable from those found for $\hbar\omega = 1$ meV. Thus, there is no noticeable dispersion in the magnetic excitations near (π,π) between $\hbar\omega = 1$ and 5 meV.

We have also performed higher-resolution measurements of $S(Q,\omega)$ to gain confidence in the magnetic cross section suggested by Fig. 2. Because of prohibitively large counting times, a complete survey as in Fig. 3 was not possible. However, we have collected two important scans along $(\pi,\bar{\pi})$, namely, through the middle and along the edge of the square with vertices $(\pi,\pi) \pm \delta(0,\pi)$ and $\pm\delta(\pi,0)$ for $\hbar\omega = 1$ and 0.65 meV. The dashed and dotted lines in Fig. 1 represent these scans. Figure 4 shows the results for $\hbar\omega = 1$ meV, along with the model functions, of the four-Gaussian type described above, which best fit the data. The signal is generally higher on the side ($q_x = 0.9$) of the square than through the middle ($q_x \cong 1.0$). In addition, there are clear intensity dips at the middle ($q_x = 0$) of the edge scans. It is thus obvious again that the incommensurate wave vector characterizing the magnetic fluctuations in $La_{1.925}Sr_{0.075}CuO_4$ has equal components parallel and perpendicular to the ordering vector for pure La_2CuO_4. The values for ξ and δ obtained from fitting the lower-T and higher-resolution data at $\hbar\omega = 1$ meV (Fig. 4) and 0.65 meV are indistinguishable from those obtained from the data of Fig. 3.

In addition to showing low-T data, Fig. 4 displays scans at 100 K. Clearly, the well-resolved double-peak structure becomes a broad maximum centered at (π,π). Beyond showing that the incommensurate $\hbar\omega = 1$ meV fluctuations are largely destroyed by heating to 100 K, the data demonstrate the absence of spurious (i.e., nonmagnetic) contributions, apart from a flat background, to the spectra. The solid lines through the data points are the outcome of a fit to the sum of four Gaussians centered at the wave vectors $(\pi,\pi) \pm \delta(\pi,0)$ and $\pm\delta(0,\pi)$, with δ fixed at its low-temperature value, 0.14. The fitted widths correspond to $\xi = 12.7 \pm 1.7$ Å $= (3.3 \pm 0.4)a_0$, implying that correlated regions (with areas ξ^2) of spins are half as large at 100 K as at $T \leq 12$ K. Obviously, a single broad Gaussian, centered at (π,π) and corresponding to even smaller correlated regions, could describe the data just as well.

All of the data discussed so far were collected for $\hbar\omega \leq 5$ meV and $x = 0.075$. For reasons of sample size

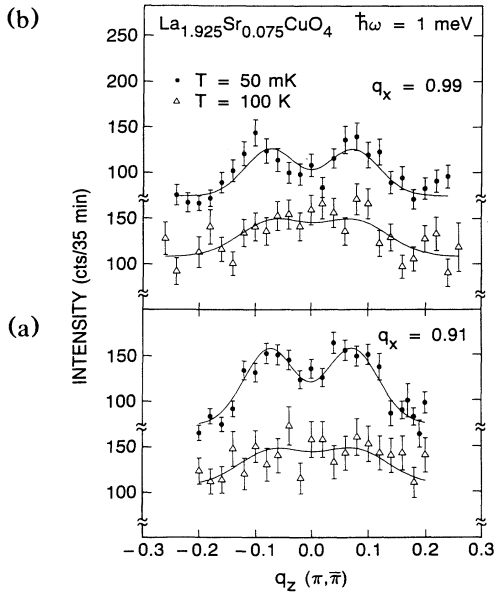

FIG. 4. Constant $\hbar\omega = 1$ meV scans collected at two temperatures for fixed $q_x = 0.9$ [frame (a)] and $q_x = 1$ [frame (b)]. The incident energy was fixed at 8.09 meV and the collimations from reactor to detector were 40′-60′-60′-120′. Solid lines represent theoretical cross sections described in text.

and signal level, it is more convenient to use two-axis spectroscopy [6] to measure the magnetic fluctuations in our $x=0.14$ crystal. There, the energy transfer $\hbar\omega < E_i$ (fixed incident energy 18.5 meV) is unspecified and, owing to the two-dimensional nature of the magnetic fluctuations in $La_{2-x}Sr_xCuO_4$, the scattering cross section $d\sigma/d\Omega$ is a rough measure of the equal-time correlation function when the CuO_2 planes are perpendicular to the outgoing wave vector $\mathbf{k}_f$. Figure 2(b) shows data taken as a function of q_x with this condition satisfied. At $q_x \cong 0.88$ and 1.14, there are well-resolved peaks above background. Because the in-plane momentum transfers in Fig. 2(b) are offset along $(\pi,\bar{\pi})$ by approximately $q_z=0.14$, the data show that as for $x=0.075$, the incommensurate peaks occur at wave vectors of the form $(\pi,\pi)\pm\delta(\pi,0)$ and $\pm\delta(0,\pi)$. Indeed, we are able to describe the $x=0.14$ data using the four-Gaussian form successfully applied to the $x=0.075$ data. The solid line in Fig. 1(b) represents the resolution and background corrected cross section which best describes the data. The corresponding incommensurability $\delta=0.24\pm0.01$, while the correlation length $\xi=17\pm4$ Å $=(4.5\pm1)a_0$. Just as for the $x=0.075$ sample, warming to 100 K makes the incommensurate peaks for $x=0.14$ unresolvable. Assuming δ to be fixed at its 12-K value, the fitted correlation length ξ drops to $8.4\pm1.4=(2.2\pm0.4)a_0$.

Figure 1 summarizes the overall outcome of this experiment, frame (a) showing the locations (solid circles) of the incommensurate wave vectors characterizing the magnetic fluctuations and (b) giving the wave numbers δ and inverse correlation lengths $K=\kappa^{-1}$ for the incommensurability. The vectors $\boldsymbol{\delta}$ are along $(0,\pi)$ and $(\pi,0)$, as for the spin-density waves obtained in Fermi surface nesting and domain-wall scenarios for the Hubbard model with $U/t\lesssim4$ [1]. Because $\delta\cong2x$ [Fig. 1(b)], the wavelength for the instability is approximately a_0/x, which is shorter than the predicted wavelengths [1] by at least a factor of 2. Larger U/t ($\gtrsim4$) does not improve the agreement between theory [1] and experiment because the prediction here is that $\boldsymbol{\delta}\|(\pm\pi,\pm\pi)$. There are other proposals, notably for spiral states [2] and staggered flux phases [3], which give $\boldsymbol{\delta}$ along $(\pi,0)$ and $(0,\pi)$, but might simultaneously yield $\delta>x$. It is worth emphasizing, however, that Monte Carlo calculations [13] on the single-band Hubbard model give no evidence for δ's larger than those obtained from the analytic spin-density-wave theories [1]. Another approach to the problem is to neglect many-body effects and consider the magnetic susceptibility associated with the full one-electron band structure of $La_{2-x}Sr_xCuO_4$. From existing literature [14], $\chi''(Q,\omega)$ obtained in this way peaks along the $(\pm\pi,\pm\pi)$ directions. We conclude that given present theoretical results, neither the one-band Hubbard model nor first-principles one-electron band structure for metallic $La_{2-x}Sr_xCuO_4$ account satisfactorily for our data [15].

We have performed the first determination of the wave vectors [Figs. 1(a) and 1(b)] and correlation lengths [Fig. 1(b)] for the incommensurate magnetic fluctuations in metallic $La_{2-x}Sr_xCuO_4$. The correlation length ξ does not depend strongly on x, and for $x=0.14$ is considerably longer than the spacing between holes in the CuO_2 planes. It is also of the same order as the pair coherence length for superconducting $La_{1.85}Sr_{0.15}CuO_4$. At 100 K, ξ is reduced to such an extent that the incommensurate peaks are replaced by a broad maximum centered at (π,π).

We are grateful to J. Als-Nielsen and J. Kjems for their hospitality and encouragement at Risø, the Danish Research Academy and U.S. Department of Energy for funding at Risø, Oak Ridge (Contract No. DE-AC05-840R21400) and Los Alamos National Laboratories. It is also a pleasure to thank O. Andersen, P. Lee, P. Littlewood, W. Pickett, B. Shraiman, and J. Zaanen for helpful conversations, R. Currat and S. Pujol for valuable assistance and advice at the ILL, B. Batlogg for excellent suggestions and susceptibility data, and H. Hwang for transport measurements. T.E.M. acknowledges the financial support of NSERC.

[1] R. J. Jelitto, Phys. Status Solidi (b) **147**, 391 (1988); H. J. Schultz, Europhys. Lett. **4**, 1609 (1987); M. Inui and P. Littlewood (to be published); T. Giamarchi and C. Lhuillier, Phys. Rev. B **42**, 10641 (1990); J. Zaanen and O. Gunnarsson, Phys. Rev. B **40**, 7391 (1989); J. P. Lu *et al.*, Phys. Rev. Lett. **65**, 2466 (1990).

[2] B. I. Shraiman and E. D. Siggia, Phys. Rev. Lett. **62**, 1564 (1989); S. John and P. Voruganti (to be published); C. L. Kane *et al.*, Phys. Rev. B **41**, 2653 (1990).

[3] T. C. Hsu, J. B. Marston, and I. Affleck, Phys. Rev. B **43**, 2866 (1991).

[4] See, e.g., G. Shirane *et al.*, Phys. Rev. B **41**, 6547 (1990); J. Rossat-Mignod *et al.* (to be published).

[5] S. M. Hayden *et al.*, Phys. Rev. Lett. **66**, 821 (1991).

[6] T. R. Thurston *et al.*, Phys. Rev. B **40**, 4585 (1989); G. Shirane *et al.*, Phys. Rev. Lett. **63**, 330 (1989); R. J. Birgeneau *et al.*, Phys. Rev. B **38**, 6614 (1988).

[7] H. Takagi *et al.*, Phys. Rev. B **40**, 2254 (1989); K. Sun *et al.*, Phys. Rev. B **43**, 239 (1991).

[8] C. H. Chen *et al.* (unpublished).

[9] B. Batlogg (unpublished).

[10] D. R. Harshman *et al.*, Phys. Rev. B **38**, 852 (1988); A. Weidinger *et al.*, Phys. Rev. Lett. **62**, 102 (1988).

[11] D. Vaknin *et al.*, Phys. Rev. Lett. **58**, 2802 (1987).

[12] G. Aeppli *et al.*, Phys. Rev. Lett. **62**, 2052 (1989); R. R. P. Singh *et al.*, Phys. Rev. Lett. **62**, 2736 (1989).

[13] See review by D. J. Scalapino, in *High Temperature Superconductivity* (Addison-Wesley, Redwood City, 1990).

[14] W. F. Pickett, H. Krakauer, and R. E. Cohen, Physica (Amsterdam) **165&166B**, 1055 (1990); J. M. Xu *et al.*, Phys. Lett. A **120**, 489 (1987).

[15] Motivated by the present experiment, two groups [P. Littlewood and J. Zaanen, and Y. Zha, Q. Si, and K. Levin (private communications)] have shown that a three-band tight-binding model with appropriately chosen parameters (which vary with x) can yield the incommensurate vectors $\boldsymbol{\delta}$ found in our experiment.

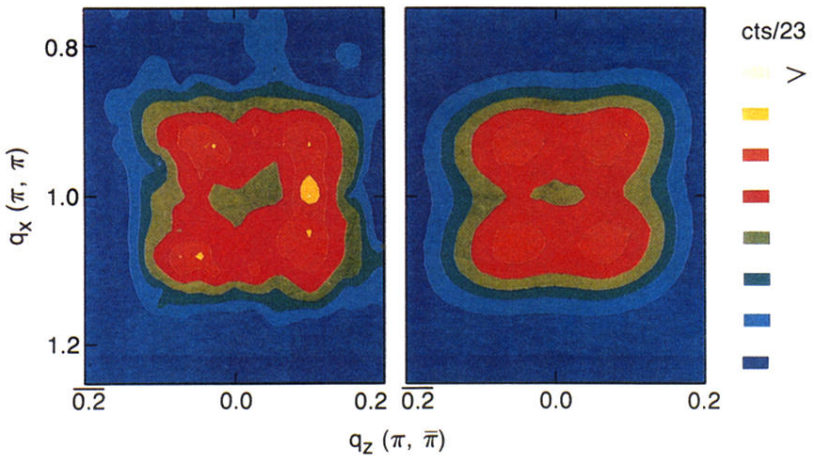

FIG. 3. Contour plots of background-corrected scattering (left) collected at fixed $\hbar\omega = 1$ meV for $x = 0.075$ with spectrometer configuration specified in the caption of Fig. 2(a), and the resolution-corrected theoretical cross section (right) which best describes the data.